Study of the Potts model on the honeycomb and triangular lattices: Low-temperature series and partition function zeros

1998 J. Phys. A: Math. Gen. 31 2287

(http://iopscience.iop.org/0305-4470/31/10/007)

J. Phys. A: Math. Gen. **31** (1998) 2287–2310. Printed in the UK PII: S0305-4470(98)87772-X

Study of the Potts model on the honeycomb and triangular lattices: Low-temperature series and partition function zeros

Heiko Feldmann†§, Anthony J Guttmann‡‖, Iwan Jensen‡¶, Robert Shrock†+ and Shan-Ho Tsai†*

† Institute for Theoretical Physics, State University of New York, Stony Brook, NY 11794-3840, USA

‡ Department of Mathematics and Statistics, The University of Melbourne, Parkville, Vic 3052, Australia

Received 24 September 1997

Abstract. We present and analyse low-temperature series and complex-temperature partition function zeros for the q-state Potts model with $q = 4$ on the honeycomb lattice and $q = 3, 4$ on the triangular lattice. A discussion is given on how the locations of the singularities obtained from the series analysis correlate with the complex-temperature phase boundary. Extending our earlier work, we include a similar discussion for the Potts model with $q = 3$ on the honeycomb lattice and with $q = 3, 4$ on the kagomé lattice.

1. Introduction

The two-dimensional (2D) q-state Potts models citepotts,wurev for various q have been of interest as examples of different universality classes for phase transitions and, for $q = 3, 4$, as models for the adsorption of gases on certain substrates. Unlike the $q = 2$ (Ising) case, however, for $q \geqslant 3$, the free energy has never been calculated in closed form for arbitrary temperature. It is thus of continuing value to obtain further information about the 2D Potts model. It has long been recognized that a very powerful method for doing this is via the calculation and analysis of series expansions for thermodynamic quantities such as the specific heat, magnetization, and susceptibility [3]. For $q = 2, 3$, and 4, the respective 2D q-state Potts ferromagnets have continuous phase transitions, and the critical singularities and associated exponents are known exactly [2, 4, 5]. Recently, two of us have calculated and analysed long low-temperature series expansions for the Potts model with $q = 3$ on the honeycomb lattice and for the Potts model with $q = 3$ and $q = 4$ on the kagomé lattice [6]. These have been used to make very precise estimates of the respective critical points, to confirm a formula for the honeycomb lattice and to strengthen a previous refutation of an old conjecture for the kagomé lattice. The other three authors have recently used a relation between complex-temperature (CT) properties of the Potts model on a given lattice

§ E-mail address: feldmann@insti.physics.sunysb.edu
‖ E-mail address: tonyg@maths.mu.oz.au
¶ E-mail address: iwan@maths.mu.oz.au
+ E-mail address: shrock@insti.physics.sunysb.edu
* E-mail address: tsai@insti.physics.sunysb.edu

0305-4470/98/102287+24$19.50

and physical properties of the Potts antiferromagnet (AF) on the dual lattice to rule out other conjectures [7] and have calculated CT zeros of the partition function for these three cases of q and lattice type [8]. The study of properties of spin models with the magnetic field and temperature generalized to complex values was pioneered by Yang and Lee [9] for the magnetic field and Fisher for the temperature [10]. Some of the earliest work on CT properties of spin models dealt with zeros of the partition function [10–12]. Another major reason for early interest in CT properties of spin models was the fact that unphysical, CT singularities complicated the analysis of low-temperature series expansions to obtain information about the location and critical exponents of the physical phase transition [13].

Here we shall present a unified study of the Potts model on the honeycomb lattice for $q = 4$ and on the triangular lattice for $q = 3$ and $q = 4$. For each q value and lattice type, our results include (i) long, low-temperature series for the specific heat, spontaneous magnetization, and initial susceptibility derived using the finite-lattice method [14, 15], extended by noting the structure of the correction terms [16]; (ii) a calculation of the CT zeros and, from these, an inference about the CT phase boundary; and (iii) a discussion of how the positions of the physical and unphysical singularities extracted from the series analysis correlate with the CT phase boundary. Since both the critical exponents and the location of the paramagnetic-to-ferromagnetic (PM–FM) phase transition are known exactly for these models, we shall focus mainly on obtaining new information on CT properties from the series and CT zeros. Using the results of [6–8], we shall also discuss subject (iii) for the Potts model with $q = 3$ on the honeycomb lattice and $q = 3$ and 4 on the kagomé lattice. It is useful to perform a unified analysis of this type because, aside from well-understood exceptions†, the physical and CT singularities of the thermodynamic functions lie on the continuous locus of points $\mathcal{B}$ which serves as the boundaries of the CT phases‡; consequently, an approximate knowledge (or exact knowledge, if available) of where this boundary lies is of considerable help in checking which CT singularities that one extracts from a series analysis are trustworthy and which are not. This will be discussed further below. Note that low-temperature series on the honeycomb lattice correspond to high-temperature series on the triangular lattice, and vice versa.

2. Model

The (isotropic, nearest-neighbour) q-state Potts model at temperature T on a lattice Λ is defined by the partition function

$$Z = \sum_{\{\sigma_n\}} \mathrm{e}^{-\beta\mathcal{H}} \tag{2.1}$$

with the Hamiltonian

$$\mathcal{H} = J \sum_{\langle nn' \rangle} (1 - \delta_{\sigma_n \sigma_{n'}}) + H \sum_n (1 - \delta_{0\ \sigma_n}) \tag{2.2}$$

where $\sigma_n = 0, \ldots, q-1$ are $\mathbb{Z}_q$-valued variables on each site $n \in \Lambda$, $\beta = (k_B T)^{-1}$, and $\langle nn' \rangle$ denotes pairs of nearest-neighbour sites. The symmetry group of the Potts Hamiltonian

† The free energy also has an isolated singularity at $|K| = \infty$ and (see theorem 6 of [17]) for the Ising model on lattices with odd coordination number a singularity at $z = -1$. The latter lies on the CT phase boundary for the honeycomb lattice but is isolated for the heteropolygonal $3 \cdot 12^2$ lattice.

‡ As discussed in [18] the CT extension of a physical phase is obtained by analytically continuing the free energy from the interval of physical temperature to a maximal region allowed by nonanalytic boundaries. Henceforth we shall generally take the adjective 'CT extension' as implicit when referring to phases. There are also other CTs that have no overlap with any physical phase; we shall denote these by O for 'other'.

is the symmetric group on q objects, S_q. We use the notation $K = \beta J, h = \beta H$,

$$a = z^{-1} = \mathrm{e}^{K} \tag{2.3}$$

$$x = \frac{\mathrm{e}^{K} - 1}{\sqrt{q}} \tag{2.4}$$

and

$$\mu = \mathrm{e}^{-2H}. \tag{2.5}$$

(The variable z was denoted u in [6].) The (reduced) free energy per site is denoted as $f = -\beta F = \lim_{N_s \to \infty} N_s^{-1} \ln Z$, where N_s denotes the number of sites in the lattice. There are actually q types of external fields which one may define, favouring the respective values $\sigma_n = 0, \ldots, q-1$; it suffices for our purposes to include only one. The order parameter (magnetization) is defined to be

$$m = \frac{qM - 1}{q - 1} \tag{2.6}$$

where $M = \langle \sigma \rangle = \lim_{h \to 0} \partial f / \partial h$. With this definition, $m = 0$ in the S_q-symmetric, disordered phase, and $m = 1$ in the limit of saturated ferromagnetic (FM) long-range order. Finally, the (reduced, initial) susceptibility is denoted as $\bar{\chi} = \beta^{-1}\chi = \partial m / \partial h|_{h=0}$. We consider the zero-field model, $H = 0$, unless otherwise stated. For $J > 0$ and the dimensionality of interest here, $d = 2$, the q-state Potts model has a phase transition from the symmetric, high-temperature paramagnetic (PM) phase to a low-temperature phase involving spontaneous breaking of the S_q symmetry and onset of FM long-range order. This transition is continuous for $2 \leqslant q \leqslant 4$ and first-order for $q \geqslant 5$. As noted above, the model has the property of duality [1, 2, 19, 20], which relates the partition function on a lattice Λ with temperature parameter x, to another on the dual lattice with temperature parameter

$$x_d \equiv \mathcal{D}(x) = \frac{1}{x} \qquad \text{i.e. } a_d \equiv \mathcal{D}(a) = \frac{a + q - 1}{a - 1}. \tag{2.7}$$

Other exact results include formulae for the PM–FM transition temperature on the square, triangular, and honeycomb lattices [1, 20], and calculations of the free energy at the phase-transition temperature, and of the related latent heat for $q \geqslant 5$ [21]. The case $J < 0$, i.e. the Potts AF, has also been of interest because of its connection with graph colorings. Depending on the type of lattice and the value of q, the antiferromagnetic (AFM) model may have a low-temperature phase with AFM long-range order. Alternatively, it may not have any finite-temperature PM–AFM phase transition but instead may exhibit nonzero ground-state entropy. For the Potts model on the honeycomb lattice, the well known $q = 2$ (Ising) case [22, 23] falls into the former category, while the model with $q \geqslant 3$ falls into the latter category [24, 25] with nonzero ground-state entropy [25–28]. Reviews of the model include [2, 29].

For the q-state Potts model, from duality and a star-triangle relation, together with a plausible assumption of a single transition, one can derive algebraic equations that yield the PM–FM critical points for the honeycomb (hc) and triangular (t) lattices [20]. The equation for the honeycomb lattice is

$$x^3 - 3x - \sqrt{q} = 0 \qquad \text{i.e. } a^3 - 3a^2 - 3(q-1)a - q^2 + 3q - 1 = 0 \text{ (honeycomb)} \tag{2.8}$$

and, as follows from equation (2.7), the corresponding formula for the triangular lattice is obtained by the replacement $x \to 1/x$:

$$\sqrt{q}x^3 + 3x^2 - 1 = 0 \qquad \text{i.e. } a^3 - 3a + 2 - q = 0 \text{ (triangular).} \tag{2.9}$$

It will be useful to have the explicit solutions for the cases studied here. For $q = 4$ on the honeycomb lattice, equation (2.8) reduces to $(a-5)(a+1)^2 = 0$, yielding the PM–FM critical point

$$a_{\mathrm{hc,\ PM\text{–}FM},q=4} = z^{-1}_{\mathrm{hc,\ PM\text{–}FM},q=4} = 5 \tag{2.10}$$

together with a double root at the CT value

$$a_{\mathrm{hc},2,q=4} = z^{-1}_{\mathrm{hc},2,q=4} = -1. \tag{2.11}$$

For $q = 3$ on the triangular lattice, equation (2.9) has the solutions

$$a_{\mathrm{t},1,q=3} = a_{\mathrm{t,\ PM\text{–}FM},q=3} = \cos(2\pi/9) + \sqrt{3}\sin(2\pi/9) = 1.879\,385\ldots \tag{2.12}$$

i.e. $z_{\mathrm{t,\ PM\text{–}FM},q=3} = 0.532\,0889\ldots$,

$$a_{\mathrm{t},2,q=3} = \cos(2\pi/9) - \sqrt{3}\sin(2\pi/9) = -0.347\,296\ldots \tag{2.13}$$

and

$$a_{\mathrm{t},3,q=3} = -2\cos(2\pi/9) = -1.532\,089\ldots. \tag{2.14}$$

For $q = 4$, equation (2.9) reduces to $(a-2)(a+1)^2 = 0$, so that the physical PM–FM critical point is given by

$$a_{\mathrm{t},1,q=4} = a_{\mathrm{t,\ PM\text{–}FM},q=4} = 2 \tag{2.15}$$

and there is a double root at the CT value

$$a_{\mathrm{t},2,q=4} = -1. \tag{2.16}$$

3. Series expansions

The low-temperature series expansion is based on perturbations from the fully aligned ground state and is expressed in terms of the low-temperature variable z and the field variable $y = 1 - \mu$. Details of the methods can be found in [6], so here it suffices to say that in order to derive series in z for the specific heat, magnetization and susceptibility one need only calculate the expansion in y to second order, i.e.

$$Z = Z_0(z) + yZ_1(z) + y^2Z_2(z) \tag{3.1}$$

where $Z_k(z)$ is a series in z formed by collecting all terms in the expansion of Z containing factors of y^k. We use the finite-lattice method [15] to approximate the infinite-lattice partition function Z by a product of partition functions $Z_{m,n}$ on *finite* $(m \times n)$ lattices, with each $Z_{m,n}$ calculated by transfer-matrix techniques. As explained in [6], this leads to a series in z correct to order $w_s(m-2) + m - 1$, where w_s is the maximal number of sites contained within the largest width w of the rectangles, and m is the number of nearest neighbours of each site. The implementation of the algorithm on the honeycomb lattice [6] has $w_s = 2w$ and $m = 3$. The triangular lattice is represented as a square lattice with additional interactions along one of the diagonals, and in this case $w_s = w$ and $m = 6$. In addition, we make use of a recent extension procedure discussed in [16], which allows us to calculate additional series terms.

The extension procedure for the 4-state Potts model on the honeycomb lattice is the same as for the 3-state model [6]. For a given width the expansion is correct to order $2w + 2$, and we calculated the series up to $w = 12$. Next we look at the integer sequences

Table 1. Low-temperature series for the 4-state honeycomb lattice Potts model magnetization ($m(z) = \sum_n m_n z^n$), susceptibility ($\bar{\chi}(z) = \sum_n x_n z^n$), and specific heat ($\bar{C}(z) = \sum_n c_n z^n$).

n	m_n	x_n	c_n
0	1	0	0
1	0	0	0
2	0	0	0
3	−4	6	54
4	−12	36	144
5	−60	234	900
6	−220	1 284	2 916
7	−936	6 804	14 112
8	−4 092	38 160	59 616
9	−17 840	198 912	280 908
10	−80 868	1 070 316	1 304 100
11	−356 172	5 499 054	5 974 254
12	−1 640 872	29 005 692	28 501 416
13	−7 433 604	149 318 838	133 160 508
14	−34 541 160	776 570 508	641 771 424
15	−159 080 304	3 987 307 152	3 037 720 320
16	−743 832 276	20 560 750 344	14 671 207 872
17	−3 469 487 112	105 345 948 384	70 242 548 778
18	−16 321 682 424	540 305 120 844	340 125 653 664
19	−76 796 957 940	2 761 471 319 562	1 640 652 533 460
20	−363 235 185 312	14 111 436 147 228	7 963 315 328 520
21	−1 720 415 299 660	71 964 766 006 350	38 614 602 921 930
22	−8 176 521 038 556	366 780 011 157 360	187 903 674 109 404
23	−38 925 659 520 072	1 866 864 944 056 032	914 552 556 040 350
24	−185 771 131 129 720	9 495 487 987 576 116	4 460 734 444 147 344
25	−888 069 677 637 192	48 251 046 682 543 824	21 771 823 449 345 750
26	−4 253 549 708 242 236	245 022 903 414 632 628	106 415 060 736 772 476
27	−20 404 302 611 163 396	1 243 326 018 023 082 990	520 535 130 747 734 844
28	−98 033 976 216 116 940	6 305 270 741 929 760 652	2 548 904 536 404 499 392
29	−471 655 884 252 852 348	31 956 599 345 155 563 546	12 490 681 376 369 529 306
30	−2272 238 036 173 908 576	161 878 582 502 746 522 164	61 260 473 924 462 872 080

$d_s(w)$ obtained by taking the difference between the expansions obtained from successive widths w,

$$Z_{w+1}(z) - Z_w(z) = z^{2w+3} \sum_{s \geqslant 0} d_s(w) z^s. \tag{3.2}$$

In this case the formulae for the correction terms are simply given by polynomials of order $2s + k$. We managed to find formulae for the first four correction terms, which enabled us to calculate the series for the specific heat C, magnetization m, and susceptibility $\bar{\chi}$ to order 30. The resulting series for m, $\bar{\chi}$, and the (reduced) specific heat $\bar{C} = C/(k_B K^2)$ are given in table 1.

The extension procedure for the triangular lattice is essentially the same as for the honeycomb lattice. The only difference is that the order of the polynomials is $s + k$. For a given width the expansion is correct to order $4w + 5$, and we calculated the series up to $w = 14$ for $q = 3$ and up to $w = 12$ for $q = 4$. We found formulae for the first seven or eight correction terms in the case $q = 3$ and the first six or seven correction terms for $q = 4$. The series were thus derived to order 69 (60) for the specific heat and magnetization

and to order 68 (59) for the susceptibility in the case $q = 3$ ($q = 4$). The resulting series for m, $\bar{\chi}$, and the (reduced) specific heat $\bar{C} = C/(k_B K^2)$ are given in tables 2 and 3.

4. Analysis of series

4.1. Honeycomb lattice, $q = 4$

We have analysed the series using dlog Padé approximants (PAs) and differential approximants (DAs); for a general review of these methods, see [3]. We first comment on the physical PM–FM phase transition. The series yield a value for the critical point in excellent agreement with the known value $z_{\mathrm{hc,\ PM\text{–}FM},q=4} = \frac{1}{5}$. For example, the differential approximants of the type $[L/M_0, M_1]$ with $L = 1$ and $L = 2$ to the specific-heat series yield $z_{\mathrm{hc,\ PM\text{–}FM},q=4} = 0.199\,93(4)$ and $0.199\,91(5)$, while those for the magnetization yield $0.199\,99(3)$ and $0.200\,05(7)$, respectively, with similarly good agreement for other values of L and for the approximants to the susceptibility. Concerning the critical exponents at this transition, the value $q = 4$ is the borderline between the interval $2 \leqslant q \leqslant 4$ where this transition is second order and the interval $q > 4$ where it is first order. Related to this, the $q = 4$ 2D Potts model has the special feature that the thermodynamic functions have strong confluent logarithmic corrections to their usual algebraic scaling forms [4] at the PM–FM transition (on any lattice). For example, the singularities in the specific heat and magnetization are $C_{\mathrm{sing}} \sim |t|^{-2/3}(-\ln|t|)^{-1}$ for $t \to 0$, where $t = (T - T_c)/T_c$, and $M_{\mathrm{sing}} \sim (-t)^{1/12}(-\ln|t|)^{-1/8}$ for $t \to 0^-$. Consequently, simple fits of the series to an algebraic singularity without this confluent logarithmic correction are not expected to agree well with the known singularities. Indeed, this was the general experience in early series work, and the same is found for the longer series here. As an illustration, a naive fit to a simple algebraic singularity for the specific heat would yield the value $\alpha' \sim 0.5$ rather than the known value $\alpha' = \frac{2}{3}$. Since these confluent singularities may also affect singularities at CT points, it could be useful in future work, as was noted earlier for the square-lattice model [30], to carry out a more sophisticated analysis of the series including these confluent singularities. However, because our primary focus here is on obtaining new information on CT properties rather than reproducing exactly known results for the critical exponents of the physical PM–FM singularity, and because it is not known if the confluent logarithmic corrections do affect the CT singularities, we have not tried to include such logarithmic factors in fits to the CT singularities.

Proceeding to CT singularities, we find evidence for one on the negative real z axis at

$$z_{\mathrm{hc},\ell,q=4} = -0.33(1) \qquad \text{i.e. } a_{\mathrm{hc},\ell,q=4} = -3.0(1). \tag{4.1}$$

Here the subscript ℓ stands for 'leftmost' singularity on the negative real axis. We shall present below, as an application of the mapping discussed in [7], an analytic derivation of the exact value $a_{\mathrm{hc},\ell,q=4} = -3$. Clearly, the value extracted from the series analysis is in excellent agreement with the exact determination. By the mapping of [7], it follows that the singularity in the specific heat at this point $a_{\mathrm{hc},\ell,q=4}$, as approached from larger negative a, i.e. smaller negative z, is the same as the singularity in the specific heat of the $q = 4$ Potts AF on the triangular lattice at the $T = 0$ critical point as approached from finite temperature.

We also find evidence from the series analyses for at least one complex conjugate (cc) pair of singularities. One such pair is observed at

$$z_{\mathrm{hc,cc1},q=4},\ z^*_{\mathrm{hc,cc1},q=4} = 0.02(2) \pm 0.38(1)\mathrm{i}. \tag{4.2}$$

Table 2. Low-temperature series for the 3-state triangular lattice Potts model magnetization ($m(z) = \sum_n m_n z^n$), susceptibility ($\bar{\chi}(z) = \sum_n x_n z^n$), and specific heat ($\bar{C}(z) = \sum_n c_n z^n$).

n	m_n	x_n	c_n
0	1	0	0
1	0	0	0
2	0	0	0
3	0	0	0
4	0	0	0
5	0	0	0
6	−3	2	72
7	0	0	0
8	0	0	0
9	0	0	0
10	−18	24	600
11	−18	24	726
12	24	−20	−1 440
13	0	0	0
14	−171	366	7 056
15	−162	324	8 100
16	153	−42	−13 824
17	252	−312	−20 808
18	−1 704	4 788	94 176
19	−2 106	6 036	119 130
20	1 998	−1 356	−196 800
21	2 586	−1 820	−291 942
22	−14 364	54 036	917 664
23	−28 098	99 252	1 986 924
24	19 008	−3 024	−2 389 248
25	43 020	−53 352	−5 092 500
26	−147 024	686 988	10 788 960
27	−317 304	1 382 336	26 041 338
28	125 775	285 870	−21 643 104
29	612 954	−926 172	−81 270 876
30	−1 370 868	7 988 984	111 771 360
31	−3 909 528	19 975 392	369 058 596
32	907 209	6 245 886	−215 519 232
33	7 487 136	−12 161 464	−1 109 316 384
34	−11 849 868	89 970 804	975 825 840
35	−46 762 686	273 568 968	5 032 861 050
36	252 159	134 393 334	−1 479 323 520
37	95 554 296	−181 279 824	−15 448 628 352
38	−101 751 129	1 023 192 774	7 864 780 656
39	−543 365 058	3 619 881 892	65 059 375 680
40	−122 514 741	2 436 896 022	−501 168 000
41	1 155 684 132	−2 347 049 916	−204 974 863 146
42	−703 522 230	10 960 701 972	30 675 861 720
43	−6 365 905 992	47 574 029 772	839 928 958 800
44	−2 758 467 240	39 732 936 192	205 816 597 536
45	13 464 222 858	−27 776 348 840	−2 605 531 430 700
46	−2 746 064 529	113 242 596 582	−499 814 655 264
47	−73 051 066 008	609 802 710 144	10 503 247 729 086
48	−49 228 732 689	624 311 338 494	5 545 501 277 184
49	154 702 726 236	−310 099 907 604	−32 529 619 836 714
50	27 843 506 676	1 118 687 211 276	−16 889 519 112 000
51	−824 524 729 038	7 680 614 520 344	127 594 218 106 044

Table 2. (Continued)

n	m_n	x_n	c_n
52	−769 717 612 998	9 376 180 586 412	106 385 351 442 240
53	1 712 690 965 746	−2 931 391 777 128	−391 772 958 832 758
54	1 028 360 456 820	10 088 397 834 056	−346 803 904 520 640
55	−9 179 822 752 182	95 352 726 717 060	1 514 773 303 324 380
56	−11 186 857 401 165	136 258 369 372 986	1 772 276 306 524 416
57	18 287 963 891 184	−19 982 241 659 216	−4 555 690 872 068 178
58	19 778 864 095 701	79 744 569 755 022	−5 942 932 736 977 104
59	−99 841 772 973 294	1 162 198 685 059 320	17 371 599 040 182 528
60	−155 837 562 896 784	1 933 440 869 909 764	27 467 732 378 426 400
61	186 952 834 687 950	15 265 872 471 072	−51 015 725 275 014 492
62	315 816 183 555 867	459 254 636 055 438	−92 730 567 932 042 472
63	−1 058 267 389 015 764	13 930 030 719 657 636	191 575 464 300 372 474
64	−2 095 009 390 517 868	26 811 413 231 763 564	403 304 437 878 595 584
65	1 783 741 344 539 292	4 261 574 859 846 552	−541 403 899 076 919 450
66	4 604 880 525 574 113	−285 699 911 125 030	−1366 060 254 075 157 608
67	−10 852 791 490 392 174	164 052 498 128 398 560	2008 868 679 625 758 660
68	−27 404 067 162 573 072	364 675 626 055 119 000	5689 560 499 409 542 368
69	15 230 158 436 520 024		−5331 645 029 087 453 988

The central values correspond to $a_{\mathrm{hc,cc1},q=4}$, $a^*_{\mathrm{hc,cc1},q=4} = 0.14 \pm 2.6\mathrm{i}$. As we shall show later, this pair of singularities is consistent with lying on the CT phase boundary $\mathcal{B}$.

4.2. Triangular lattice, $q = 3$

The series yield values for the PM–FM critical point in excellent agreement with the exactly known expression, equation (2.12). For example, the first-order DAs of the form $[L/M_0, M_1]$ with $L = 1$ for the free energy yield $z_{\mathrm{t,\ PM\text{–}FM},q=3} = 0.532\,095(85)$, in complete agreement, to within the uncertainty, with the known value given by equation (2.12). For reference, the thermal and field exponents for the 2D $q = 3$ Potts model are $y_{\mathrm{t}} = \frac{6}{5}$ and $y_{\mathrm{h}} = \frac{28}{15}$, so that the critical exponents for the specific heat, magnetization, and susceptibility are $\alpha = \alpha' = \frac{1}{3}$, $\beta = \frac{1}{9}$, and $\gamma = \gamma' = \frac{13}{9} = 1.444\ldots$ [2, 5]. The above approximants yield the exponent $\alpha' = 0.331(27)$, again in agreement with the known value. Similar statements apply to the magnetization and susceptibility.

Concerning CT singularities, the series for m and $\bar{\chi}$ indicate a singularity on the negative real axis, at $z_{\mathrm{t},-,q=3} \simeq -0.71$ and $z_{\mathrm{t},-,q=3} \simeq -0.65$. If we assume that this is, as it should be, the same singularity, and average the positions, we obtain

$$z_{\mathrm{t},-,q=3} \equiv z_{\mathrm{t},\ell,q=3} = -0.68(5) \tag{4.3}$$

or equivalently,

$$a_{\mathrm{t},\ell,q=3} = -1.47(11) \tag{4.4}$$

where the numbers in parentheses are our estimates of the theoretical uncertainties. We observe that our numerical determination in equation (4.4) is consistent, to within the uncertainty, with being equal to the value given by the root in equation (2.14), hence our use of the symbol $a_{\mathrm{t},\ell,q=3}$ in equation (4.4).

We find a complex-conjugate pair of singularities at

$$z_{\mathrm{t},e,q=3},\ z^*_{\mathrm{t},e,q=3} = 0.0209(1) \pm 0.531(1)\mathrm{i}. \tag{4.5}$$

Table 3. Low-temperature series for the 4-state triangular lattice Potts model magnetization ($m(z) = \sum_n m_n z^n$), susceptibility ($\bar{\chi}(z) = \sum_n x_n z^n$), and specific heat ($\bar{C}(z) = \sum_n c_n z^n$).

n	m_n	x_n	c_n
0	1	0	0
1	0	0	0
2	0	0	0
3	0	0	0
4	0	0	0
5	0	0	0
6	−4	3	108
7	0	0	0
8	0	0	0
9	0	0	0
10	−24	36	900
11	−48	72	2 178
12	60	−72	−3 672
13	0	0	0
14	−300	711	14 112
15	−480	1080	27 000
16	144	144	−18 432
17	1392	−2556	−114 444
18	−4392	12 852	290 628
19	−7248	230 04	467 856
20	2904	−504	−354 600
21	13 280	−21 192	−1 479 114
22	−27 348	122 877	1 768 536
23	−142 512	525 996	12 073 896
24	29 948	69 366	−5 861 808
25	241 872	−531 576	−29 193 750
26	−336 072	1 970 154	22 900 176
27	−1 711 936	7 833 756	165 214 728
28	−950 268	6 613 164	64 153 152
29	4 759 680	−12 953 124	−654 007 014
30	−2 790 212	24 243 261	163 350 540
31	−25 599 600	137 623 572	2 795 893 038
32	−17 648 472	130 318 974	1 579 935 744
33	53 777 216	−138 059 232	−8 670 448 116
34	24 551 472	115 953 372	−6 567 077 628
35	−385 317 888	2 338 653 528	48 371 018 850
36	−379 526 360	2 854 976 280	42 263 145 144
37	757 341 312	−2 039 815 332	−136 194 436 566
38	678 358 092	433 835 991	−156 222 316 800
39	−4 605 291 200	33 211 423 320	620 105 092 776
40	−8 295 782 520	62 346 454 416	1 141 035 505 200
41	9 858 368 640	−23 201 806 140	− 2 037 399 494 436
42	16 985 972 056	−32 015 102 700	−3 672 631 070 136
43	−59 595 025 824	499 277 941 344	8 580 306 247 938
44	−136 999 873 260	1 118 920 518 738	21 031 881 323 904
45	81 105 525 424	49 166 169 540	−21 085 184 576 700
46	365 702 657 748	−1 181 015 194 617	−81 272 696 605 524
47	−702 809 980 704	6 981 782 741 964	105 969 879 959 940
48	−2310 592 067 252	20 279 205 891 438	391 533 801 047 712
49	494 570 429 328	6 051 532 683 060	−199 750 003 201 224
50	5981 082 924 792	−22 190 276 278 656	−1 418 750 008 893 000
51	−6198 365 886 016	84 541 391 331 996	823 212 895 965 966

Table 3. (Continued)

n	m_n	x_n	c_n
52	−37 809 130 736 064	354 875 036 323 788	7 044 054 404 212 800
53	−6 090 856 346 112	205 839 844 753 932	−409 244 046 301 098
54	97 187 254 024 404	−407 434 833 461 367	−24 496 576 650 092 484
55	−39 928 634 332 608	984 502 454 280 336	1 572 414 830 767 440
56	−562 081 834 061 556	5 754 184 442 187 300	112 350 099 811 614 336
57	−340 608 212 779 056	5 393 530 501 373 556	50 948 011 956 216 330
58	1482 012 248 480 712	−6 542 615 994 118 038	−401 080 749 409 250 964
59	283 544 734 049 040	8 894 396 469 832 452	−181 847 403 757 220 400
60	−8231 813 619 904 556		1752 211 155 816 298 440

From our analysis of the respective series, we infer the following values of singular exponents at the points (4.5):

$$(\alpha', \beta, \gamma')_{z_{\mathrm{t},e,q=3}} = (1.19(1),\ -0.18(1),\ 1.17(1)). \tag{4.6}$$

The central values in equation (4.5) correspond to

$$a_{\mathrm{t},e,q=3},\, a^*_{\mathrm{t},e,q=3} = 0.0740 \pm 1.88\mathrm{i}. \tag{4.7}$$

From the CT zeros to be discussed below, we see clearly that the complex conjugate members of this pair are endpoints of arcs of CT zeros of Z, corresponding to continuous arcs of singularities of the free energy in the thermodynamic limit. (This type of correspondence with endpoints on $\mathcal{B}$ is indicated by the subscripts e here and in other cases below.) In passing, we observe that the exponent values in equation (4.6) are not too different from the respective exponents obtained from the series analysis of [31] for the singularities $u_s = -0.301\,939(5) \pm 0.378\,7735(5)\mathrm{i}$ in the 2D spin-1 Ising model on the square lattice, namely [31] $(\alpha', \beta, \gamma') = (1.1693(3), -0.1690(2), 1.1692(2))$. The complex conjugate pair of points u_s is analogous to the pair in equation (4.7) because the members of this pair were shown [32] to be endpoints of arcs of CT zeros protruding into the CT extension of the FM phase of the spin-1 square-lattice Ising model. We also observe that the values of both these sets of exponents are consistent with the equality $\alpha' = \gamma'$. However, we already know that such an equality, even if it were to hold for these cases, is not a general result for singular exponents at endpoints of arcs of a CT boundary $\mathcal{B}$ protruding into the CT extension of the FM phases for a spin model. A counter-example is provided by the (isotropic, spin $\frac{1}{2}$) Ising model on the triangular lattice. In this case, one can determine the CT phase diagram exactly, and $\mathcal{B}$ consists of the union of the unit circle $|u + \frac{1}{3}| = \frac{2}{3}$ and the semi-infinite line segment $-\infty \leqslant u \leqslant -\frac{1}{3}$ [33], where $u = z^2$. Thus, in this case there is an exactly known analogue to the arc endpoints, namely, the endpoint at $u_e = -\frac{1}{3}$ (where the subscript e denotes 'endpoint') of the line segment protruding into the CT extension of the FM phase. An analysis of low-temperature series [34] had earlier yielded the inference that $\gamma'_e = \frac{5}{4}$, while exact results [33] yielded $\alpha'_e = 1$ (and $\beta_e = -\frac{1}{8}$), so that $\alpha'_e \neq \gamma'_e$.

We find a second complex conjugate pair at

$$z_{\mathrm{t},e',q=3},\, z^*_{\mathrm{t},e',q=3} = -0.515(3) \pm 0.322(3)\mathrm{i} \tag{4.8}$$

with exponents $(\alpha', \beta, \gamma') = (1.2(1), -0.25(10), 1.2(1))$. The central values in equation (4.8) correspond to

$$a_{\mathrm{t},e',q=3},\, a^*_{\mathrm{t},e',q=3} = -1.40 \pm 0.873\mathrm{i}. \tag{4.9}$$

This pair is consistent with lying on the CT phase boundary, as will be discussed below. It should be noted that we would not expect the low-temperature series to be sensitive to the third root, $a_{t,2,q=3}$, of equation (2.9), since this root is masked by the nearer singularity $a_{t,3,q=3}$ (that is, $z_{t,3,q=3} = -0.652\,704\ldots$ is closer to the origin in the z plane than $z_{t,2,q=3} = -2.879\,385\ldots$).

4.3. Triangular lattice, $q = 4$

For the physical PM–FM critical point of the $q = 4$ Potts model on the triangular lattice, the discussion that we gave above for the honeycomb lattice applies; that is to say, the position of the physical singularity is well approximated, but the critical exponents are not, due to the presence of confluent logarithms. For CT properties, we first note that the series do not give a firm indication of a singularity on the negative real axis. We find a complex-conjugate pair of singularities at

$$z_{t,e,q=4},\ z^*_{t,e,q=4} = 0.0304(2) \pm 0.498(2)\mathrm{i}. \tag{4.10}$$

We have also studied the exponents at this pair of singularities. If one assumes that there are no strong confluent singularities present, such as the logarithms that are present at the physical critical point, then from our series analysis we extract the following values, with their quoted uncertainties:

$$(\alpha', \beta, \gamma')_{z_{t,e,q=4}} = (1.18(2), -0.17(2), 1.20(2)). \tag{4.11}$$

However, we caution that it is not known whether strong confluent singularities are present at the points (4.10), and if they are, then the values in equation (4.11) would have a lower degree of reliability. The central values in equation (4.10) correspond to

$$a_{t,e,q=4},\ a^*_{t,e,q=4} = 0.122 \pm 2.00\mathrm{i}. \tag{4.12}$$

As in the $q = 3$ case, from the CT zeros to be presented below, we see clearly that the complex conjugate members of this pair of singularities are endpoints of arcs of CT zeros of Z.

We find a second complex conjugate pair at

$$z_{t,e',q=4}, z^*_{t,e',q=4} = -0.461(5) \pm 0.281(5)\mathrm{i}. \tag{4.13}$$

The central values correspond to

$$a_{t,e',q=4}, a^*_{t,e',q=4} = -1.58 \pm 0.964\mathrm{i}. \tag{4.14}$$

Again, this pair can be associated with endpoints of arcs of zeros, as is especially clear from figure 7. There is also some sign of another pair of singularities in the vicinity of $z \simeq -0.2 \pm 0.6\mathrm{i}$, corresponding to $a \simeq -0.5 \pm 1.5\mathrm{i}$. The members of this complex conjugate pair are consistent with lying on the CT phase boundary. It is possible that there are also other complex conjugate pairs of singularities.

5. Complex-temperature zeros

5.1. General

The (zero-field) Potts model partition function Z for a finite lattice is, up to a possible prefactor, a polynomial in the Boltzmann weight a. We calculate this polynomial by standard transfer-matrix methods. From this, we then compute the zeros. In the thermodynamic limit, via a coalescence of zeros, there forms a continuous locus $\mathcal{B}$ of points where the free energy

is nonanalytic. As was noted, this locus serves as the union of boundaries of the various CT phases [18] and, aside from well-understood exceptions [17], the CT singularities of thermodynamic functions occur on the continuous locus of points $\mathcal{B}$ where the free energy is nonanalytic, since it is analytic in the interior of physical phases and their CT extensions. Thus, calculations of CT zeros on sufficiently large finite lattices yield useful information on the CT phase diagram in the thermodynamic limit. Hence, when investigating CT singularities, it is useful to do so in conjunction with a calculation of the CT zeros of the partition function to infer the approximate location of the CT phase boundary $\mathcal{B}$.

To illustrate this, let us return briefly to the $q = 2$ Ising special case of the Potts model, for which both the free energy [22] and the magnetization [23] are known exactly. We recall that the expression for the spontaneous magnetization is [23]

$$M = \frac{(1+u)^{1/4}(1-6u+u^2)^{1/8}}{(1-u)^{1/2}} \tag{5.1}$$

where $u = z^2$ in the FM phase and the CT extension of it (with $M = 0$ elsewhere). Let us pretend that we did not know the exact free energy or magnetization, but that we had a low-temperature (small-u) series for M and analysed it using dlog PAs. We would find singularities at the following four points: (i) $u_{\rm PM-FM} = 3 - 2\sqrt{2}$, the physical PM–FM phase-transition point; (ii) $u_{\rm PM-AFM} = u_c^{-1} = 3 + 2\sqrt{2}$, the PM–AFM transition point; (iii) $u = -1$ and (iv) $u = 1$. This shows the value and importance of analysing CT singularities of thermodynamic functions from series expansions; these can give one deeper knowledge of the exact functions. Indeed, in this illustrative example, a dlog Padé analysis of the series for M would enable us to reconstruct the exact analytic expression for this quantity. The knowledge of the CT zeros and corresponding CT phase diagram give complementary information, in particular, information on which of the singularities found from the series analysis occur in the true thermodynamic function. Thus, from calculations of CT zeros for finite lattices, we could determine the approximate CT phase boundaries, and, in particular, the CT extension of the FM phase. We would then infer that this (CT) FM phase does not include the point $3 + 2\sqrt{2}$, so that the second apparent singularity extracted from the series does not occur in the true function M, since the low-temperature series only apply in the physical FM phase and its CT extension. Even without the CT zeros, in this case, we would also know that the apparent singularity at $u = 1$ does not occur in the true M, since M is certainly zero, and all thermodynamic functions are analytic, at the infinite-temperature point $u = 1$ (and since this point is clearly in the PM phase, the low-temperature series are again not applicable in its vicinity). This example thus illustrates the value of both the study of CT singularities from series expansions and CT zeros of the partition function. Here, of the four apparent singularities extracted from the series, only two, namely the physical critical point (i) and the CT singularity (iii) are true singularities of M, since the others occur in regions outside the CT extension of the FM phase where the series applies. In this exactly solved case, these results are obvious, but the lesson holds more generally and illustrates the usefulness of having at least approximate knowledge of the CT phase boundary of a given model when analysing series expansions to obtain locations of CT singularities. Note that all of the CT singularities occur on the locus of points $\mathcal{B}$ where the free energy is nonanalytic, which in this case is a limaçon of Pascal (given by equations (2.17) and (2.18) in [18], the image in the u plane of the circles [10] $|z \pm 1| = \sqrt{2}$ in the z plane). This is also a general feature (with the exception noted in theorem 6 of [17]) and constitutes another reason for the value that a knowledge of CT zeros and the corresponding locus $\mathcal{B}$ have for series analyses and vice versa.

As a technical remark, we note that the problem of calculating the zeros of the partition

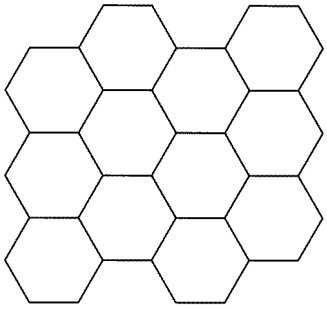

Figure 1. Honeycomb lattice to illustrate our conventions for indicating sizes.

function for large lattices is a challenging one, since the degree of the polynomial is equal to the number of bonds, $N_b = (\Delta/2)N_s$, where Δ is the coordination number, N_s is the number of sites, and there is a very large range in the sizes of the coefficients, from q for the highest-degree term a^{N_b} to exponentially large values for intermediate terms. The latter property is obvious from the fact that for $K = 0$, i.e. $a = 1$, the sum of the coefficients in Z is q^{N_s}. A general property of the CT phase boundary for any lattice and q value is invariance under complex-conjugation: $\mathcal{B} \to \mathcal{B}$ as $a \to a^*$. For previous calculations of CT zeros for the Potts model on the triangular and square lattices, see [35, 36, 30, 29].

The CT zeros are equivalently plotted in the complex a or z plane; we shall plot them in the a plane because the resultant figures are somewhat more compact and because this maintains conformity with the plots for the square lattice, where the $\mathrm{Re}\,(a) > 0$ part of the phase boundary is very simple (either exactly or approximately part of a circle, depending on boundary conditions).

In making inferences about the CT phase boundary $\mathcal{B}$ in the thermodynamic limit from calculations on CT zeros on finite lattices, it is important to get an idea of the effects of different boundary conditions (BCs) and lattice sizes. Accordingly, in [8], the authors performed calculations with three different BCs and compared the resultant CT zeros with the exactly known CT phase boundary for the $q = 2$ Ising model on the honeycomb and kagomé lattices. This also served as a check on the computer programs used. We shall use the same three types of BCs here, and we identify them next, following the notation of [8].

5.2. Honeycomb lattice, $q = 4$

Before we start to present our results, we have to introduce our notation for the sizes and orientations of the lattices. To indicate the size of a given lattice, we count the number of hexagons. As an illustration, the size of the honeycomb lattice in figure 1 is 4×3 hexagons. The number of sites in a lattice is also dependent on the BCs: with periodic boundary conditions in the horizontal direction for example, the sites on the left and right are identified, while with free BCs they are counted independently of each other.

Since we make use of duality in this work, we use lattices that have a corresponding dual lattice. This excludes lattices that are periodic in both directions, for the following reason: duality relies on the fact that every closed polygon divides the lattice into at least two regions. However, a lattice with periodic BCs in both directions, and hence with toroidal geometry, has the property that one can easily draw a closed contour that does not divide the surface into two disjunct regions. Since boundary effects are, in general, best suppressed if one uses periodic BCs in as many directions as possible, we use BCs that

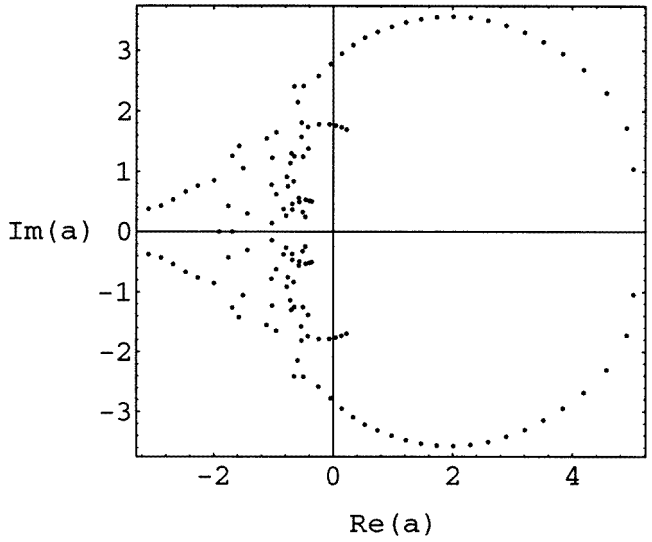

Figure 2. CT zeros of Z in the a plane for the $q = 4$ Potts model on a honeycomb lattice of size 7×6 hexagons and BCs of type (fbc,pbc).

are periodic in one direction and free in the other. Our notation for the BCs is (fbc,pbc) for free and periodic BCs in the horizontal (x) and vertical (y) directions, respectively (see figure 1), and (pbc,fbc) for periodic and free BCs in the x and y directions. Note that for the (fbc,pbc) choice, there is one site per hexagon at the boundary with only two instead of the usual $\Delta = 3$ bonds. For the (pbc,fbc) BCs, there are two of these sites per boundary hexagon. This motivated the formulation of a third kind of boundary condition [8]: starting from the (pbc, fbc) BCs, one adds bonds connecting the boundary sites with fewer than three bounds so that all sites on the lattice have the same coordination number $\Delta = 3$. This type of boundary condition is denoted as $(\mathrm{pbc,fbc})_\Delta$. In [8], a comparison was made with the Ising case $q = 2$ where the CT phase boundary is exactly known, and it was found that (for the same lattice sizes as are used here) the CT zeros calculated with all three types of BCs, tracked the exactly known CT phase boundary reasonably well. In particular, the $(\mathrm{pbc,fbc})_\Delta$ choice produced CT zeros with, in general, the least scatter. The (fbc,pbc) choice also exhibited the special feature that a subset of zeros lay exactly on a certain circular arc comprising part of $\mathcal{B}$.

We show our calculations of the CT zeros of the $q = 4$ Potts model on the honeycomb lattice, using the above three types of BCs, in figures 2–4. The zeros cross the positive real a axis at only one point, which is the PM–FM transition point; this value is in good agreement with the exact result $a_c = 5$ of equation (2.10). The zeros thus exclude a PM–AFM transition and associated low-temperature phase with AFM long-range order, since such a transition would be represented by a curve of CT zeros crossing the real a axis at some point in the interval $0 \leqslant a < 1$. Concerning earlier work that bears on this, we note that a recent Monte Carlo study of the $q = 3$ Potts AF on the honeycomb lattice [25] yielded evidence that that model has no symmetry-breaking phase transition and thus is disordered at all temperatures, including $T = 0$, where it exhibits nonzero ground state entropy measured to be $S_0/k_B = 0.957$. The latter value is close to an estimate [25] from earlier large-q series [26] and is bracketed closely by rigorous upper and lower bounds [28]. Because increasing q makes the spins 'floppier', one expects that the Potts AF on the

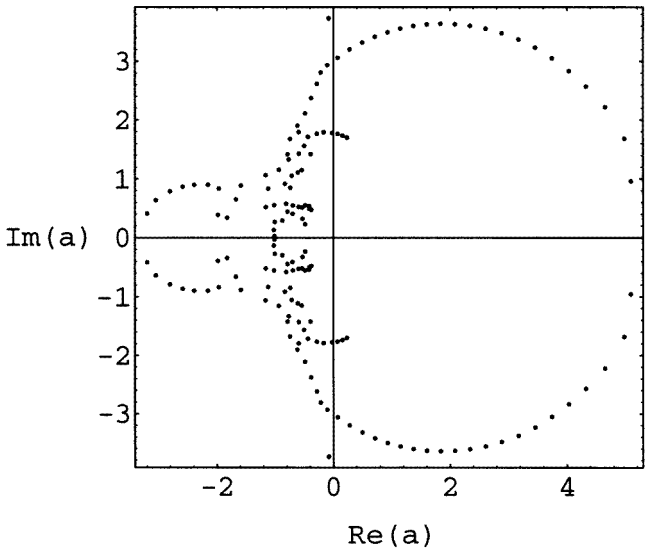

Figure 3. CT zeros of Z for the $q = 4$ Potts model on a honeycomb lattice of size 8×6 hexagons and BCs of type (pbc,fbc).

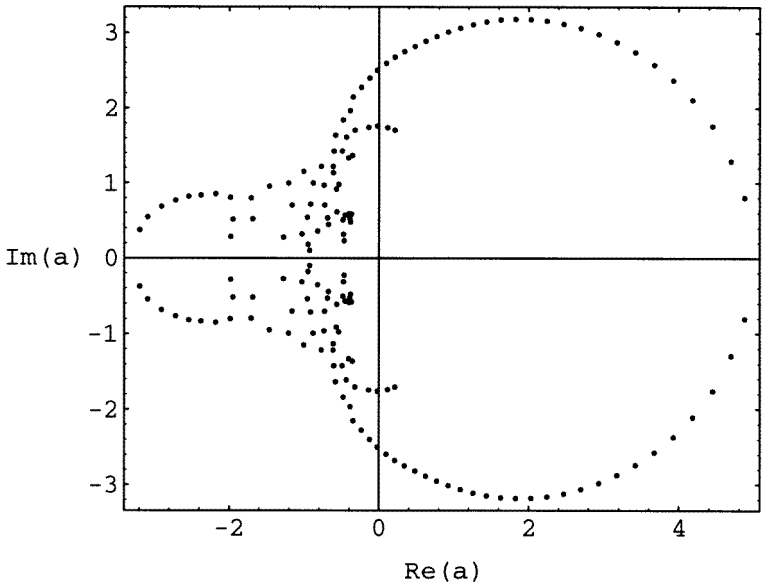

Figure 4. CT zeros of Z for the $q = 4$ Potts model on a honeycomb lattice of size 8×6 hexagons and BCs of type $(\text{pbc,fbc})_{\triangle}$.

honeycomb lattice for $q \geqslant 4$ is similarly disordered at all temperatures, and, indeed, this has been rigorously proved [24].

A second remark is that the zeros are also consistent with the inference that a curve on the CT phase boundary $\mathcal{B}$ crosses the real axis at the value in equation (2.11), $a = -1$. This crossing is clearest with the (pbc,fbc) BCs, shown in figure 3. Two other possible crossings

occur at $a = -2.0(2)$ and $a = -0.47(5)$. For the latter point we have another source of information, using duality; if a crossing did occur at this point, it would be the closest, on the left, to the origin of the a plane and consequently its dual image would be the leftmost crossing of the CT phase boundary of the $q = 4$ Potts model on the triangular lattice, in the a_d plane. In the other cases of q value and lattice type where such Potts-model series have been calculated and analysed [6], they have been able to locate the leftmost singularity on the real a axis (corresponding to the nearest singularity left of the origin in the z plane) with good accuracy. However, the analysis of the low-temperature series for the $q = 4$ Potts model on the triangular lattice does not yield very strong evidence for such a singularity.

The leftmost crossing, in the a plane, of the CT zeros for the $q = 4$ Potts model on the honeycomb lattice, and hence of $\mathcal{B}$ in the thermodynamic limit, is related by duality to physical properties of the $q = 4$ Potts AF on the dual, i.e. triangular, lattice; as discussed in [7], the full temperature interval $0 \leqslant a_d \leqslant 1$ of the q-state Potts AF on this dual lattice Λ_d maps in a 1–1 manner, under duality, to the CT interval $-\infty \leqslant a \leqslant -(q-1)$ of the Potts model on the lattice Λ. Now, it has been argued [37] that the Potts AF on the triangular lattice has a zero-temperature critical point (see also [38], where a study of the closely related $T = 0$ critical point of the $q = 3$ Potts AF on the kagomé lattice is given). Using the duality connection [7], one then deduces that the leftmost crossing of $\mathcal{B}$ for the $q = 4$ Potts model on the honeycomb lattice is at

$$a_\ell = -3. \tag{5.2}$$

The CT zeros that we have calculated are consistent with this. The slight flaring out of the zeros to the left of this point appears as a finite lattice-size effect.

As was the case with the $q = 2$ Ising case and with $q = 3$, we again observe complex-conjugate arcs of zeros protruding into, and terminating in, the CT extension of the PM phase, ending at

$$a_{\mathrm{hc},e,q=4}, a^*_{\mathrm{hc},e,q=4} = 0.27(3) \pm 1.68(4)\mathrm{i}. \tag{5.3}$$

We recall that in the exactly known $q = 2$ case, these arc endpoints occur at $a = \mathrm{e}^{\pm\pi\mathrm{i}/3}$; as discussed in [8], as q increases, these arc endpoints in the CT PM phase move to larger magnitudes $|a_e|$ and larger values of the angle $\theta = \arg(a_e)$. There also appears to be another complex conjugate pair of arcs protruding into the CT PM phase, with endpoints at

$$a_{\mathrm{hc},e',q=4}, a^*_{\mathrm{hc},e',q=4} = -0.34(3) \pm 0.45(7)\mathrm{i}. \tag{5.4}$$

A general observation is that all of the CT singularities obtained from the analysis of the low-temperature series are consistent with lying on the CT phase boundary $\mathcal{B}$. This clearly includes the physical PM–FM critical point $a_{\mathrm{hc,\ PM\text{–}FM},q=4} = 5$, the leftmost crossing at $a_{\mathrm{hc},\ell,q=4} = -3$, and also the complex conjugate pair given in equation (4.1). We note that (i) the crossing at $a = -1$, and the complex conjugate pairs of arc endpoints in the PM phase in equations (ii) (5.3), and (iii) (5.4) are not expected to be seen with the low-temperature series because they are not contiguous with the CT extension of the FM phase but rather are within a presumed O phase† for (i) and the CT PM phase for (ii) and (iii).

5.3. Triangular lattice, $q = 3$

In figures 5 and 6, we present calculations of CT zeros for the $q = 3$ Potts model on the triangular lattice. For consistency, we have plotted all of our zeros in the a plane; however, we note that when relating zeros of Z for the Potts model on one lattice Λ to those on the

† A complex-temperature O ('other') phase [17, 18] denotes one that has no overlap with any physical phase.

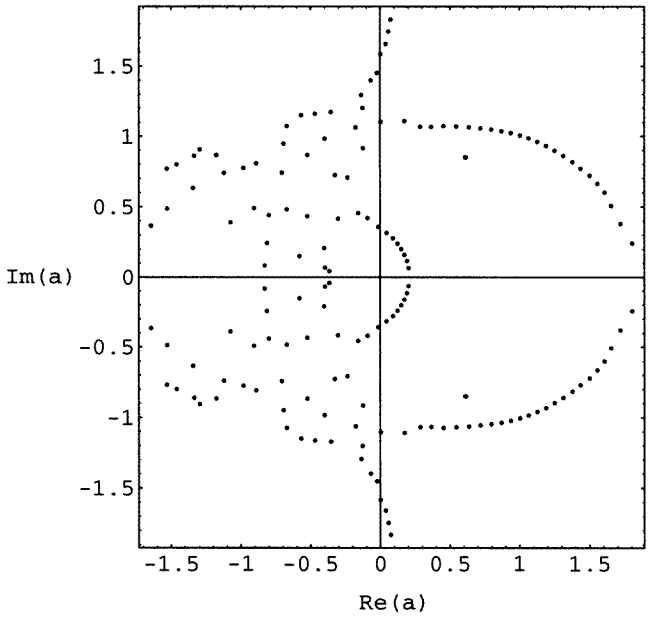

Figure 5. CT zeros of Z for the $q = 3$ Potts model on the triangular lattice, obtained via duality from a honeycomb lattice of size 8×6 hexagons and (pbc,fbc) BCs.

dual lattice Λ_d, the connection is simplest if one plots the zeros in the x plane, where x was given in equation (2.4) since in this case the duality transformation (2.7) just amounts to the inversion map $x \to 1/x$. A comparison of these figures gives a quantitative indication of the effects of different BCs. These effects are somewhat stronger for $\mathrm{Re}\,(a) < 0$ than $\mathrm{Re}\,(a) > 0$.

One observes complex-conjugate arc endpoints protruding into, and ending in, the (CT extension of the) FM phase at

$$a_e, a_e^* = 0.072(10) \pm 1.85(2)\mathrm{i}. \tag{5.5}$$

The points at which one can infer crossings of the zeros, and hence the CT phase boundary $\mathcal{B}$ are (in order, proceeding from right to left along the real a axis) (1) the PM–FM critical point $a_{\mathrm{PM-FM},q=3} = 1.879\ldots$ given by equation (2.12); (2) the PM–AFM critical point [39, 40], which has recently been measured by a Monte Carlo simulation to high precision, $a_{\mathrm{PM-AFM},q=3} = 0.203\,09(3)$ [41]; (3) $a_{2,q=3} = -0.3473\ldots$ in equation (2.13), (4) $a = -0.82(3)$, and (5) $a_{3,q=3} = -1.532\ldots$ in equation (2.14). In [35], it was suggested that points (2) and (4) were given by two of the roots of the equation $a^3 + 6a^2 + 3a - 1 = 0$, namely, $a = 0.226\,682\ldots$, $a = -0.815\,2075\ldots$, while the third root, $a = -5.411\,474\ldots$ would be associated with the completion of the complex-conjugate arcs of zeros (labelled as branches 6 in [35]) to form a closed curve crossing the negative real a axis at this root. However, neither the early [39, 40] determinations nor the recent high-precision determination [41] of $a_{\mathrm{PM-AFM}}$ agrees with the value $a = 0.226\,682$, and the suggestion about the closing of the arcs to form a closed curve crossing the negative real axis at $a = -5.411\,474$ has been refuted [7] since, by duality, it is equivalent to a finite-temperature phase transition in the $q = 3$ Potts AF on the honeycomb lattice, which is known not to occur [25]. The CT phase diagram in the a plane for the $q = 3$ Potts model on the triangular lattice thus consists of a PM, FM, and AFM phases, with indications of at least one O phase.

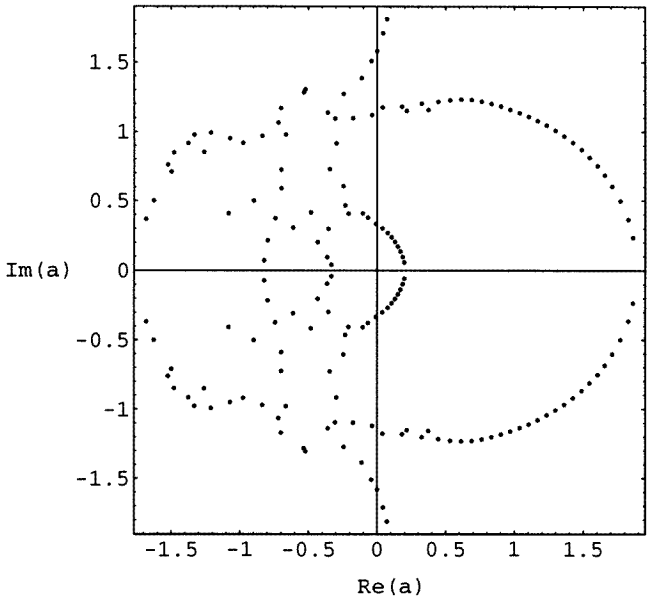

Figure 6. CT zeros of Z for the $q = 3$ Potts model on the triangular lattice, obtained via duality from results for a honeycomb lattice of size 8×6 hexagons and $(\text{pbc,fbc})_{\Delta}$ BCs.

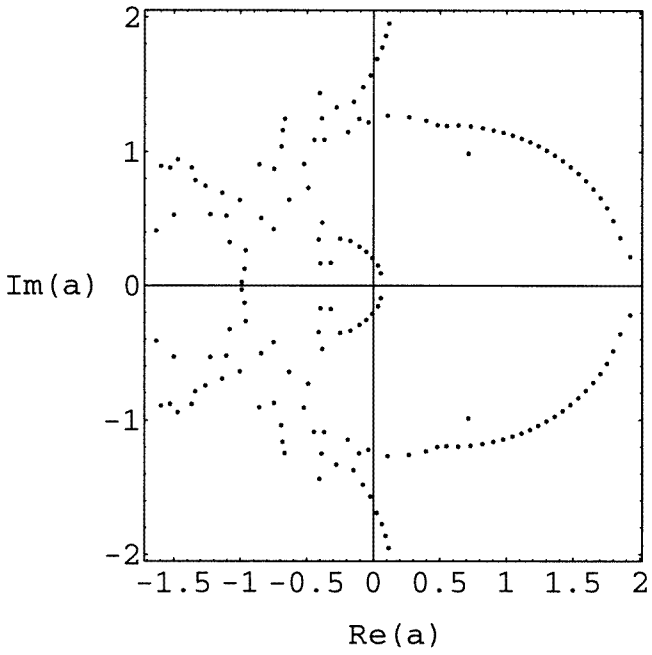

Figure 7. CT zeros of Z for the $q = 4$ Potts model on the triangular lattice, obtained via duality from a honeycomb lattice of size 8×6 hexagons and (pbc,fbc) BCs.

5.4. Triangular lattice, $q = 4$

In figures 7 and 8 we show CT zeros of the partition function for the $q = 4$ Potts model on the triangular lattice with two different sets of BCs. Qualitatively, the patterns of CT

zeros are similar to those for $q = 3$. The points at which the zeros, and hence the CT phase boundary $\mathcal{B}$ inferred in the thermodynamic limit, cross the real a axis can be obtained via duality from those for the $q = 4$ model on the honeycomb lattice. The rightmost crossing is consistent with the known exact value $a_{\mathrm{t,\ PM\text{–}FM},q=4} = 2$ in equation (2.15). This is equivalent, by duality, to the known value $a_{\mathrm{hc,\ PM\text{–}FM},q=4} = 5$ for the $q = 4$ Potts model on the honeycomb lattice. Assuming the correctness of the suggested zero-temperature critical point in the model [37], we deduce that the CT zeros and the CT phase boundary $\mathcal{B}$ have no further crossings on the positive real axis but cross this axis at $a = 0$. This would imply that in the thermodynamic limit, the innermost complex-conjugate arcs of zeros pinch together at this point. As can be seen from figures 7 and 8, this requires that the two complex-conjugate arcs of zeros nearest to the origin in the a plane must pull back slightly to the left as the lattice size goes to infinity. By duality, this crossing of the CT zeros at $a = 0$ on the triangular lattice is equivalent to the crossing of the CT zeros at $a = -3$ for the $q = 4$ Potts model on the honeycomb lattice. In the present case, the CT zeros are also consistent with the conclusion that another crossing is at $a = a_{\mathrm{t},2,q=4} = -1$, the multiple root of equation (2.9) given above in equation (2.16); the dual equivalent is that the CT zeros in the $q = 4$ Potts model on the honeycomb lattice also cross the real a axis at $a = -1$. This is, of course, consistent with our calculations of CT zeros on the honeycomb lattice. There are also suggestions of other possible crossings of CT zeros for the present $q = 4$ case on the triangular lattice. These include a possible crossing at $a = -0.33(3)$, corresponding to the observed crossing of zeros for the honeycomb lattice at $a = -2.0(2)$. We have noted above that an analysis of the low-temperature series for the $q = 4$ Potts model on the triangular lattice does not yield a firm indication of a singularity on the negative real z (equivalently a) axis. Such a singularity would occur at the leftmost crossing of the zeros, $z_\ell = a_\ell^{-1}$. It is possible that the reason for this is that, if, indeed, $a_{\mathrm{t},\ell,q=4} = -1$, then the effect of this singularity is shielded by the effects of singularities lying to the left in the complex a plane (perhaps associated with the arcs of zeros in figures 7 and 8), i.e. closer to the origin of the z plane.

We also observe clear complex conjugate arcs of zeros protruding into the FM phase, with endpoints at

$$a_{\mathrm{t},e,q=4},\ a^*_{te,q=4} = 0.12(1) \pm 1.97(3)\mathrm{i}. \tag{5.6}$$

As indicated in the notation, this complex conjugate pair of points is in very good agreement with the complex conjugate pair of singularities given in equation (4.12), identified from the analysis of the low-temperature series. Thus, in both of these cases, the $q = 3$ and $q = 4$ Potts models on the triangular lattice, we find excellent agreement between such complex conjugate pairs of singularities extracted from low-temperature series analyses and endpoints of arcs of zeros obtained from the calculation of CT zeros on finite lattices.

5.5. Comparison of CT singularities with phase boundary for triangular lattice

Evidently, the respective values of the physical PM–FM critical point $a_{\mathrm{PM\text{–}FM},q}$ and the leftmost point where $\mathcal{B}$ crosses the real a axis, $a_{\ell,q}$, as obtained from the analysis of the low-temperature series are in excellent agreement with the roots of the general formula (2.9) and also with the crossing points seen with the CT zeros for both $q = 3$ and $q = 4$. The respective complex-conjugate pair of singularities at $z_{e,q}, z^*_{e,q}$ from the analysis of the low-temperature series are seen to be the ends of complex conjugate arcs of zeros (in the thermodynamic limit, continuous arcs of singularities) protruding into and ending in the CT FM phase. For $q = 3$ and $q = 4$, from our analysis of the series we have also obtained

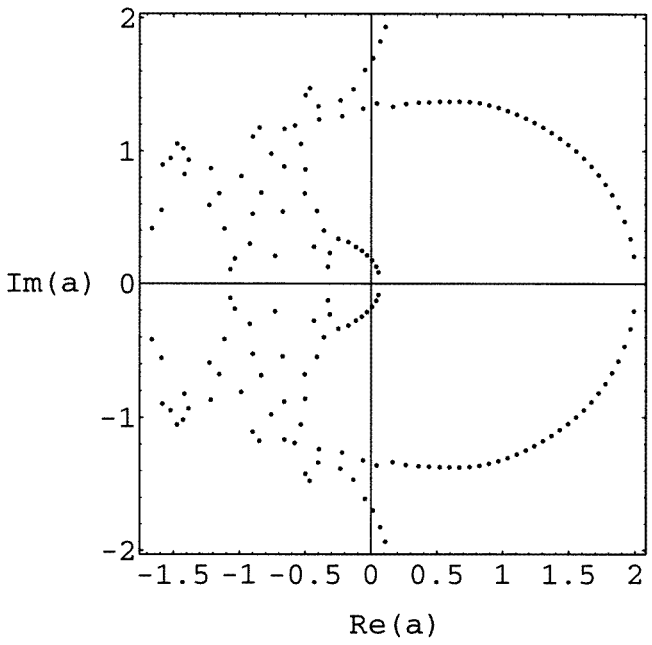

Figure 8. CT zeros of Z for the $q = 4$ Potts model on the triangular lattice, obtained via duality from a honeycomb lattice of size 8×6 hexagons and (pbc,fbc)$_\Delta$ BCs.

evidence for a complex-conjugate pair of singularities at the respective values $a_{e',q}$, $a^*_{e',q}$ as given in equations (4.9) and (4.14). Comparing these respective pairs of singularities with the CT phase boundary $\mathcal{B}$ inferred from the CT zeros for $q = 3$ and $q = 4$, we observe that each pair is consistent with lying on the respective boundary $\mathcal{B}$, in the 'northwest' and 'southwest' quadrants of the a plane.

5.6. Triangular lattice, $q = 5$

It is also of interest to present an example of CT zeros calculated for the q-state Potts model on the triangular lattice with q in the range where the Potts AF is disordered at all temperatures including $T = 0$. Accordingly, we show in figure 9 the CT zeros for the case $q = 5$. For $q > 4$, equation (2.9) has only one real root, together with a conjugate pair of complex roots. The real root for this case is $a_{\mathrm{PM-FM},q=5} = 2.103\,803\ldots$. This is in agreement with the rightmost crossing point of the zeros on the real a axis. As is evident from figure 9, the curves of zeros that we had inferred to pass through the origin for the $q = 4$ model have moved further to the left, consistent with the conclusion that no branch of $\mathcal{B}$ passes through the interval $0 \leqslant a < 1$, i.e. that the $q = 5$ Potts AF is disordered for all temperatures including $T = 0$. The other features of the CT phase diagram are similar to those that we have observed before, including the prominent complex conjugate arcs of zeros protruding into the FM phase near to the vertical axis in the a plane.

5.7. Comparison with $q = 2$ Ising case for the triangular lattice

One can gain some further insight into these results from a comparison with the exactly solved $q = 2$ Ising case. The CT phase diagram in the z plane is shown as figure 1(b) of

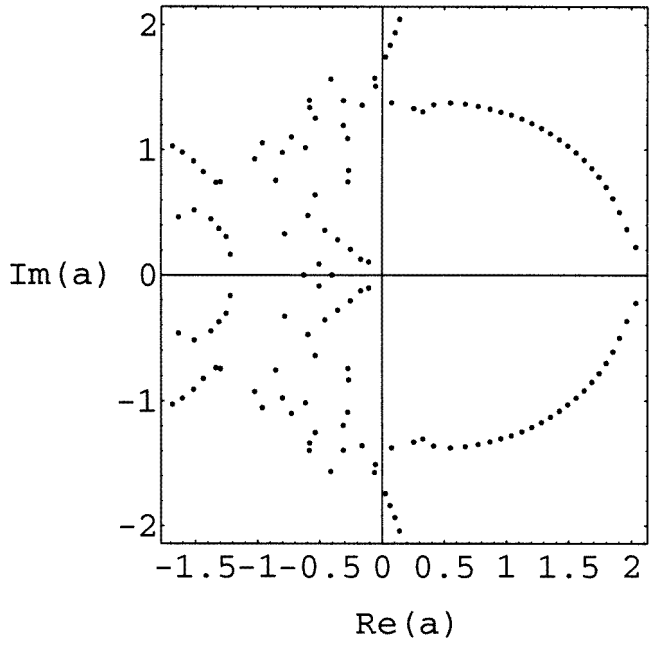

Figure 9. CT zeros of Z for the $q = 5$ Potts model on the triangular lattice, obtained via duality from a honeycomb lattice of size 7×6 hexagons and (fbc,pbc) BCs.

[33]; in the a plane, the CT phase boundary maps to the union of (i) an oval with its longer side along the real a axis, crossing this axis at $\pm a_{\mathrm{PM-FM},q=2} = \pm\sqrt{3}$, and (ii) a vertical line segment along the imaginary a axis extending from $-\sqrt{3}\mathrm{i}$ upward to $\sqrt{3}\mathrm{i}$. This line segment bisects the oval and divides the interior into the PM phase to the right and an O phase to the left; outside of the oval is the FM phase. The two components (i) and (ii) of $\mathcal{B}$ intersect at the multiple points $a = \pm\mathrm{i}$.

Now, taking the broader perspective of general q, one sees that as q increases from 2 to 4, the PM–FM phase transition point $a_{\mathrm{PM-FM},q}$, which is the largest root of equation (2.9), moves monotonically to the right, as dictated by general inequalities (as q increases, the spins become 'floppier', and one must go to lower temperature to attain FM long-range order). A qualitative change occurs as one increases q above 2, in that the middle root of equation (2.9) moves to negative values, as does this portion of the CT phase boundary. Thus, while the $T = 0$ critical point of the Ising AF corresponds to the middle root of equation (2.9), the $T = 0$ critical point of the $q = 4$ model that has been argued for does not correspond to any root of this equation (2.9).

6. Comparison of CT singularities with phase boundaries for other cases

In [8], it was noted that for the Potts model with $q = 3$ on the honeycomb lattice and with $q = 3, 4$ on the kagomé lattice, the positions of the physical PM–FM transition points, as obtained from equation (2.8) for the honeycomb lattice and from series analyses for the kagomé lattice, agreed nicely with the maximal real points at which the CT zeros crossed the real a axis. It was also noted that the leftmost crossing point of the zeros at the respective points a_ℓ were in good agreement (i) for the $q = 3$ triangular case with a prediction from

duality [7] and a precise Monte Carlo measurement of the PM–AFM transition temperature of the $q = 3$ Potts AF on the triangular lattice [41]; and (ii) for the $q = 3, 4$ kagomé case with the values obtained from low-temperature series analyses [6]. Here, we extend this comparison to the complex-a singularities.

6.1. Honeycomb lattice, $q = 3$

The low-temperature series analysis of the $q = 3$ Potts model on the honeycomb lattice in [6] yielded evidence for a complex conjugate pair of singularities in the thermodynamic functions at $z_{\pm} = -0.06(2) \pm 0.47(3)$i. The central values correspond to $a_{\pm} = -0.27 \pm 2.1$i. Comparing with the results of [8], one sees that these points lie slightly to the upper left and lower left of the curve of CT zeros in the 'northwest' and 'southwest' quadrants of the a plane. This complex conjugate pair may be associated with possible complex conjugate cusp-like structures in this vicinity, as is hinted at in figure 7 of [8].

6.2. Kagomé lattice, $q = 3$

In addition to the PM–FM critical point and the leftmost crossing point, the low-temperature series analysis of [6] found evidence for CT singularities at four complex conjugate pairs of points in the z plane, namely, $z_{1,\pm} = 0.38(2) \pm 0.24(2)$i, $z_{2,\pm} = 0.278(10) \pm 0.38(1)$i, $z_{3,\pm} = -0.113(6) \pm 0.515(10)$i, and $z_{4,\pm} = -0.37(2) \pm 0.30(5)$i. The central values correspond approximately to the points $a_{1,\pm} = 1.9 \pm 1.2$i, $a_{2,\pm} = 1.25 \pm 1.7$i, $a_{3,\pm} = -0.41 \pm 1.85$i, and $a_{4,\pm} = -1.6 \pm 1.3$i. As discussed above, one expects the true singularities of the thermodynamic functions to lie on the CT phase boundaries, since these quantities are analytic functions of complex temperature in the interiors of the CT phases. However, as our illustration with the exactly calculated magnetization of the $q = 2$ Ising case showed, low-temperature series may, in general, indicate singularities which lie off the CT phase boundary in regions where these series do not apply; the corresponding factors are presumably present in the true function (e.g. the factor $(1 - u)^{-1/2}$ in (5.1)). The poles labelled $a_{2,\pm}$ and $a_{4,\pm}$ are definitely consistent with lying on CT phase boundaries which may be plausibly inferred in the thermodynamic limit from the zeros calculated in [8] for finite lattices. For some, but not all, types of BCs, there is an indication of complex conjugate arcs of zeros protruding into the CT FM phase and ending therein at points near to $a_{4,\pm}$. The previous experience with exactly known CT phase diagrams [34, 33, 17] and a comparison between CT zeros and low-temperature series expansions for the higher-spin Ising model [31, 32] showed that, in the cases studied, the magnetization diverges at the ends of arcs or line segments of singularities of the free energy which protrude into the CT FM phase. Thus, if the complex conjugate singularities at $a_{4,\pm}$ do lie at the ends of such arcs, this would be in accord with the divergence found in the magnetization in [6]. The points $a_{3,\pm}$ lie somewhat outside the curves of zeros, in the interior of the FM phase, while the points $a_{1,\pm}$ lie slightly inside of the CT phase boundary $\mathcal{B}$ in the interior of the CT PM phase.

6.3. Kagomé lattice, $q = 4$

In this case, [6] obtained the two complex conjugate pairs of CT singularities at $z_{1,\pm} = 0.275(10) \pm 0.305(10)$i and $z_{2,\pm} = -0.345(10) \pm 0.235(1)$i. The central values correspond to the points $a_{1,\pm} = 1.63 \pm 1.81$i, and $a_{2,\pm} = -1.98 \pm 1.35$i. The complex conjugate pair $a_{1,\pm}$ lie on the inferred phase boundary $\mathcal{B}$ in the upper and lower right quadrants of the a

plane. Similarly, the complex conjugate pair $a_{2,\pm}$ lie on $\mathcal{B}$ in the upper and lower quadrants of the left-hand half plane $\mathrm{Re}\,(a) < 0$, in the region of arc-like structures on this boundary.

7. Conclusion

We have carried out a unified study of the q-state Potts model with $q = 4$ on the honeycomb lattice and with $q = 3, 4$ on the triangular lattice, including the calculation and analysis of long low-temperature series and the calculation of CT zeros of the partition function which allow us to make reasonable inferences about the CT phase boundary $\mathcal{B}$ in the thermodynamic limit. In all cases, the series are in excellent agreement with the known values of the respective PM–FM critical points. For the $q = 4$ Potts model on the honeycomb lattice, there is no PM–AFM critical point and, concerning CT properties, we find that the series analysis and CT zeros yield a value of the leftmost crossing a_ℓ in good agreement with the inference from duality and the zero-temperature critical point of the $q = 4$ Potts model on the triangular lattice, namely, $a_\ell = -3$. For the triangular lattice, the CT zeros agree well with the known PM–AFM transition of the $q = 3$ model and are also consistent with the property that the $q = 4$ model has a $T = 0$ critical point. The singularities seen in the series at the largest negative values of a are seen to be the leftmost points where the CT phase boundary crosses the negative real a axis. For both $q = 3$ and $q = 4$ the series also yield clear indications of a complex-conjugate pair of singularities which are seen to lie at the ends of arcs of CT zeros protruding into the CT FM phase. In each case, there are indications of another complex conjugate pair lying on the respective CT phase boundaries. We have also discussed how the positions of various CT singularities lying at complex values of a in this model and also in the $q = 3, 4$ model on the kagomé lattice correlate with the respective CT phase boundaries.

Acknowledgments

Financial support from the Australian Research Council is gratefully acknowledged by IJ and AJG. The research of HF, RS, and S-HT was partially supported by the US National Science Foundation under the grant PHY-97-9722101, for which these authors also express gratitude.

References

[1] Potts R B 1952 *Proc. Camb. Phil. Soc.* **48** 106
[2] Wu F Y 1982 *Rev. Mod. Phys.* **54** 235
Wu F Y 1983 *Rev. Mod. Phys.* **55** 315 (errata) (Also note that there is a misprint in table V: for $q = 4$, $\eta = \frac{1}{4}$, not $\frac{1}{2}$)
[3] Gaunt D S and Guttmann A J 1974 *Phase Transitions and Critical Phenomena* vol 3 ed C Domb and M S Green (New York: Academic)
Guttmann A J 1989 in *Phase Transitions and Critical Phenomena* vol 13 ed C Domb and M S Green (New York: Academic)
[4] Nauenberg M and Scalapino D J 1980 *Phys. Rev. Lett.* **44** 837
Cardy J L, Nauenberg M and Scalapino D J 1980 *Phys. Rev.* B **22** 2560
[5] Itzykson C, Saleur H and Zuber J-B (ed) 1988 *Conformal Invariance and Applications to Statistical Mechanics* (Singapore: World Scientific)
[6] Jensen I, Guttmann A J and Enting I G 1997 *J. Phys. A: Math. Gen.* **30** 8067
[7] Feldmann H, Shrock R and Tsai S-H 1997 *J. Phys. A: Math. Gen.* **30** L663
[8] Feldmann H, Shrock R and Tsai S-H 1998 *Phys. Rev.* E **57** 1335
[9] Yang C N and Lee T D 1952 *Phys. Rev.* **87** 404

Lee T D and Yang C N 1952 *Phys. Rev.* **87** 410
[10] Fisher M E 1965 *Lectures in Theoretical Physics* vol 7C (Colorado: University of Colorado Press) p 1
[11] Katsura S 1967 *Prog. Theor. Phys.* **38** 1415
Abe R 1967 *Prog. Theor. Phys.* **38** 322
Ono S, Karaki Y, Suzuki M and Kawabata C 1968 *J. Phys. Soc. Japan* **25** 54
[12] Abe R 1967 *Prog. Theor. Phys.* **38** 322
[13] Domb C and Guttmann A J 1970 *J. Phys. C: Solid State Phys.* **3** 1652
[14] Enting I G 1978 *J. Phys. A: Math. Gen.* **11** 563
[15] Enting I G 1996 *Nucl. Phys.* B (Proc. Suppl.) **47** 180
[16] Jensen I and Guttmann A J 1996 *J. Phys. A: Math. Gen.* **29** 3817
[17] Matveev V and Shrock R 1995 *J. Phys. A: Math. Gen.* **28** 5235
[18] Matveev V and Shrock R 1995 *J. Phys. A: Math. Gen.* **28** 1557
[19] Kihara T, Midzuno Y and Shizume T 1954 *J. Phys. Soc. Japan* **9** 681
[20] Kim D and Joseph R J 1974 *J. Phys. C: Solid State Phys.* **7** L167
Burkhardt T W and Southern B W 1978 *J. Phys. A: Math. Gen.* **11** L247
[21] Baxter R J 1973 *J. Phys. C: Solid State Phys.* **6** L445
Baxter R J, Temperley H N V and Ashley S 1978 *Proc. R. Soc. Ser. A* **358** 535
Baxter R J 1982 *J. Stat. Phys.* **28** 1
[22] Onsager L 1944 *Phys. Rev.* **65** 117
[23] Yang C N 1952 *Phys. Rev.* **85** 808
[24] Salas J and Sokal A 1997 *J. Stat. Phys.* **86** 551
[25] Shrock R and Tsai S-H 1997 *J. Phys. A: Math. Gen.* **30** 495
[26] Kim D and Enting I G 1979 *J. Combin. Theory* B **26** 327
[27] Shrock R and Tsai S-H 1997 *Phys. Rev.* E **55** 5165
[28] Shrock R and Tsai S-H 1997 *Phys. Rev.* E **55** 6791
Shrock R and Tsai S-H 1997 *Phys. Rev.* E **56** 2733
Shrock R and Tsai S-H 1997 *Phys. Rev.* E **56** 4111
[29] Martin P P 1991 *Potts Models and Related Problems in Statistical Mechanics* (Singapore: World Scientific)
[30] Matveev V and Shrock R 1996 *Phys. Rev.* E **54** 6174
[31] Enting I G, Guttmann A J and Jensen I 1995 *J. Phys. A: Math. Gen.* **27** 6987
Jensen I, Guttmann A J and Enting I G 1996 *J. Phys. A: Math. Gen.* **29** 3805
See also Jensen I and Guttmann A J 1996 *J. Phys. A: Math. Gen.* **29** 3817
[32] Matveev V and Shrock R 1995 *J. Phys. A: Math. Gen. Lett.* **28** L533
See also Matveev V and Shrock R 1995 *Phys. Lett.* A **204** 353
[33] Matveev V and Shrock R 1996 *J. Phys. A: Math. Gen.* **29** 803
[34] Guttmann A J 1975 *J. Phys. A: Math. Gen.* **8** 1236
[35] Martin P P and Maillard J-M 1986 *J. Phys. A: Math. Gen.* **19** L547
[36] Chen C N, Hu C K and Wu F Y 1996 *Phys. Rev. Lett.* **76** 169
Wu F Y, Rollet G, Huang H Y, Maillard J-M, Hu C K and Chen C N 1996 *Phys. Rev. Lett.* **76** 173
[37] Baxter R J 1987 *J. Phys. A: Math. Gen.* **20** 5241
Baxter R J 1986 *J. Phys. A: Math. Gen.* **19** 2821
[38] Kondev J and Henley C L 1996 *Nucl. Phys.* B **464** 540
[39] Grest G S 1981 *J. Phys. A: Math. Gen.* **14** L217
Saito Y 1982 *J. Phys. A: Math. Gen.* **15** 1885
[40] Enting I G and Wu F Y 1982 *J. Stat. Phys.* **28** 351
[41] Adler J, Brandt A, Janke W and Shmulyian S 1995 *J. Phys. A: Math. Gen.* **28** 5117
For an earlier series estimate see Enting I G and Wu F Y 1982 *J. Stat. Phys.* **28** 351